Proceedings of the 16th European VLBI Network Symposium
Ros, E., Benke, P., Dzib, S., Rottmann, I., & Zensus, J.A. (eds.)
September 2nd-6th 2024, Bonn, Germany

Preliminary results of identifying the g-factor of 6.7 GHz methanol maser via polarization observations

A. Kobak[1], G. Surcis[2], A. Bartkiewicz[1], M. Szymczak[1], and W. Vlemmings[3]

[1] Institute of Astronomy, Faculty of Physics, Astronomy and Informatics, Nicolaus Copernicus University, Grudziadzka 5, 87-100 Torun, Poland
[2] INAF - Osservatorio Astronomico di Cagliari, Via della Scienza 5, 09047, Selargius, Italy
[3] Department of Space, Earth and Environment, Chalmers University of Technology, 412 96, Gothenburg, Sweden

Abstract. Cosmic masers enable us to estimate the magnetic field strength via the Zeeman effect. Especially the maser emission of the OH radical, which is a paramagnetic molecule, is widely used in star-forming regions and circumstellar matter around evolved stars to measure magnetic field strengths of a few mG. The methanol molecule is instead non-paramagnetic, implying that the Zeeman splittings of its maser emissions are much smaller than the linewidth of the maser lines. Therefore, to estimate their values, a very high spectral resolution and a more careful analysis are required. Moreover, it is still unclear which of the hyperfine transitions (each with its g-factor) dominates the different maser emissions. In particular, for the 6.7 GHz methanol maser emission, the hyperfine transitions are eight. On the other hand, the Landé g-factors are undoubtedly known for all the OH maser transitions. To determine which is the dominating hyperfine transition of the 6.7 GHz methanol maser emission, we conducted simultaneous observations using the European VLBI Network of the 6.035 GHz exited OH (ex-OH) and of the 6.7 GHz methanol maser transitions towards two high-mass star-forming regions. Our earlier observations showed that these two masers arose in the two selected sources in the same spatio-kinematical regions, and both showed strongly polarized emissions. Therefore, new simultaneous observations at high-angular resolution should allow us to compare the magnetic field strength measured with the exOH with the Zeeman-splitting estimated for the methanol masers and consequently to identify the dominating hyperfine transition for the 6.7 GHz methanol maser. Here, we present preliminary results of the project EK052 that was observed in May 2023.

1. Introduction

Maser emissions are important tools for studying high-mass young stellar objects (HMYSOs). The most common one is the 6.7 GHz methanol maser emission that was discovered by Menten in 1991. This maser has been widely studied in numerous surveys (e.g., Caswell 1996, Szymczak et al. 2002, Pandian et al. 2011, Hu et al. 2016) and it greatly contributed in understanding some aspects of the formation process of high-mass stars (e.g., Ellingsen et al. 2012, Tan et al. 2014). The 6.035 GHz exited hydroxyl (hereafter ex-OH) maser emission is less common in HMYSOs (Caswell 2003, Avison et al. 2016) and appears in the late phase of HMYSO evolution (Jones et al. 2020). However, it can co-exist with the 6.7 GHz methanol maser emission under similar physical conditions (Cragg et al. 2002).

It is also known that the magnetic field can play an important role in high-mass star formation: in regulating the star formation rate, in the fragmentation process, and even in the final mass of high-mass stars (e.g., Krumholz & Federrath 2019). The maser emissions of the OH paramagnetic molecule have been widely used for estimating the magnetic field in star-forming regions and evolved stars (e.g., Szymczak et al. 2001, Hutawarakorn et al. 2002, Etoka et al. 2012, Green et al. 2015). Indeed, the Zeeman splitting between the left- and right-handed circular polarizations (LHCP and RHCP) of an OH maser emission is clearly visible and relatively easy to measure. In addition, the Landé g-factor is known for many of its maser transitions (Davies 1974, Baudry et al. 1997), making the estimation of the magnetic field from the Zeeman splitting straightforward. In the case of the 6.7 GHz methanol maser emission the estimation of the magnetic field is more difficult. Firstly, because the methanol molecule is non-paramagnetic, the Zeeman splitting is smaller than the linewidth of the maser line, and secondly, because its hyperfine structure is complex. There are eight hyperfine transitions that can possibly contribute to the 6.7 GHz maser emission, but perhaps only one dominates. Nevertheless, the values of the Landé g-factors for all these eight transitions have been theoretically estimated only recently by Lankhaar et al. (2018), but because the hyperfine transition that contributes the most to the maser emission is not known yet, the estimation of the magnetic field from the Zeeman splitting measurements is still uncertain (Surcis et al. 2019).

In this conference proceeding, we will compare the magnetic field measured from the 6.035 GHz ex-OH maser emission with the estimated Zeeman splitting of the 6.7 GHz methanol maser in two HMYSOs: W75N and ON1. Our aim is to determine the dominating hyperfine transition of the 6.7 GHz maser emission from this comparison. Our main assumption is that these two maser

emissions arise in the same volume of gas and that they are probing the same magnetic field.

2. Observations and methods

The observations were taken using the European VLBI Network (EVN) in phase-referencing and full polarization mode, on 29–30 May, 2023 towards G81.871+0.781 (known as W75N) and on 31 May–1 June, 2023 towards G69.540−0.976 (known as ON1). Each source was observed in two frequency tunings covering the exited OH 6035.092 MHz line and the methanol 6668.519 MHz line with a spectral resolution of $0.05\,\mathrm{km\,s^{-1}}$. The data were calibrated using the Astronomical Image Processing Software package (AIPS) following a standard procedure for spectral line and polarimetric observations (e.g., Surcis et al. 2022). We used J2202+4216 (BL Lac) as fringe finder, bandpass calibrator, and polarization calibrator. We used 3C286 to correct the polarization angles. We created *I*, *Q*, *U*, *RR*, and *LL* cubes for both transitions and then we produced polarization intensity, ($P_\mathrm{l} = \sqrt{Q^2+U^2}$) and polarization angle ($\chi = 0.5 \times \mathrm{atan(U/Q)}$) cubes. To identify the maser features, we followed the procedure described in Sect. 3.1 of Surcis et al. (2011).

To estimate the value of the magnetic field along the line-of-sight ($B_{||}$), we used the relation: $B_{||} = \Delta V_\mathrm{Z}/\alpha_\mathrm{Z}$; where α_Z is the Zeeman-splitting coefficient, that for the ex-OH transition is $\alpha_\mathrm{Z}^\mathrm{exOH} = 0.056\ \mathrm{m\,s^{-1}}$, and ΔV_Z is the Zeeman splitting, which for the exOH is measured as the velocity difference between the RHCP and the LHCP spectra of the same maser feature: $V_\mathrm{fit}^\mathrm{exOH}(RHCP) - V_\mathrm{fit}^\mathrm{exOH}(LHCP)$. The values of $V_\mathrm{fit}^\mathrm{exOH}$ were estimated by fitting Gaussian profiles to the RHCP and LHCP spectra. Due to the non-paramagnetic nature of the methanol molecule, in order to estimate $\Delta V_\mathrm{Z}^{meth}$, we had to use the full radiative transfer method (FRTM) code that was developed by Vlemmings et al. (2010). See, for instance, Surcis et al. (2022) for more details.

3. Results and discussion

The spectra and the spots maser distributions for both maser transitions are shown in Figures 1 and 2 for ON1 and W75N, respectively. The values of $\Delta V_\mathrm{Z}^{meth}$ and $B_{||}^\mathrm{exOH}$ as estimated from the methanol and ex-OH masers, respectively, are also indicated.

We assume that both maser transitions arise in the same volume of gas and that the probed magnetic field is the same ($B_{||}^{exOH} = B_{||}^{meth}$). Therefore, we can determine α_Z^{meth} by using

$$\alpha_\mathrm{Z}^{meth} = \frac{\Delta V_\mathrm{Z}^{meth}}{B_{||}^{exOH}}. \quad (1)$$

Comparing our estimated α_Z^{meth} with those tabled by Lankhaar et al. (2018), we aim to determine the dominant hyperfine transition of the 6.7 GHz methanol maser emission.

In the case of ON 1, for the 6.7 GHz methanol emission we measured only one Zeeman splitting of $\Delta V_\mathrm{Z}^{meth}$=3.2 $\mathrm{m\,s^{-1}}$ that is spatially close on the plane of the sky (<200 mas corresponding to <500 au at a distance of 2.57±0.34 kpc; Rygl et al. 2010) to one of the measured Zeeman pair of the ex-OH maser emission, for which we have $B_{||}^{exOH}$=−5.1 mG (Fig. 1). Therefore, from Eq. 1 we have:

$$\alpha_\mathrm{Z}^{meth,ON\ 1} = \frac{3.2\,\mathrm{m\,s^{-1}}}{-5.1\,\mathrm{mG}} = -627.45\,\mathrm{m\,s^{-1}\,G^{-1}} \quad (2)$$

This value does not coincide with any of the Zeeman coefficients tabled in Lankhaar et al. (2018) for the 6.7 GHz methanol maser emission.

A similar calculation can be done for W75N. In this case, we have two Zeeman-splitting estimates, both in the blue-shifted maser region in the north (Fig. 2). Unfortunately, there are no nearby ex-OH Zeeman pairs associated with them. The closest Zeeman pair lies at a distance of about 400 mas (corresponding to about 520 au at a distance of 1.30±0.07 kpc; Rygl et al. 2012) and is shifted in LSR velocity domain by $2.4\,\mathrm{km\,s^{-1}}$. Although the methanol and ex-OH for which we were able to make the Zeeman-splitting measurements are not coincident in space, we can assume that they both belong to the same molecular cloud and that the magnetic field is not expected to vary so much in strength. Under these assumption and following Eq. 1, we have:

$$\alpha_\mathrm{Z}^{meth,W75N} = \frac{2.1\,\mathrm{m\,s^{-1}}}{+7.32\,\mathrm{mG}} = 286.89\,\mathrm{m\,s^{-1}\,G^{-1}} \quad (3)$$

$$\alpha_\mathrm{Z}^{meth,W75N} = \frac{1.2\,\mathrm{m\,s^{-1}}}{+7.32\,\mathrm{mG}} = 163.39\,\mathrm{m\,s^{-1}\,G^{-1}} \quad (4)$$

Also in this case, the obtained values do not coincide with any of the Zeeman coefficients tabled in Lankhaar et al. (2018) for the 6.7 GHz methanol maser emission.

As one can note, we obtained three different values for α_Z^{meth} and even with opposite signs (Eqs 2–4). Moreover, according to supplementary Table 3 of Lankhaar et al. (2018), the reported theoretical values of α_Z^{meth} are at least one order of magnitude lower than the obtained values. The possible explanation is that the methanol and ex-OH masers do not arise in the same volume of gas, and the coincidence of the maser spots on the plane of the sky is only apparent. Then, the densities of the gas cloudlets might be diverse, and consequently, the local magnetic field can be different.

Next, we can try a different approach. We can estimate the magnetic field strength from the methanol maser Zeeman splitting by assuming that the hyperfine transition that shows the largest Einstein coefficient is the most favorable, as suggested by Lankhaar et al. (2018). This is the hyperfine transition $F = 3 \rightarrow 4$ ($\alpha_{\mathrm{Z}^{meth}} = -50.995\,\mathrm{m\,s^{-1}\,G^{-1}}$). Therefore, we

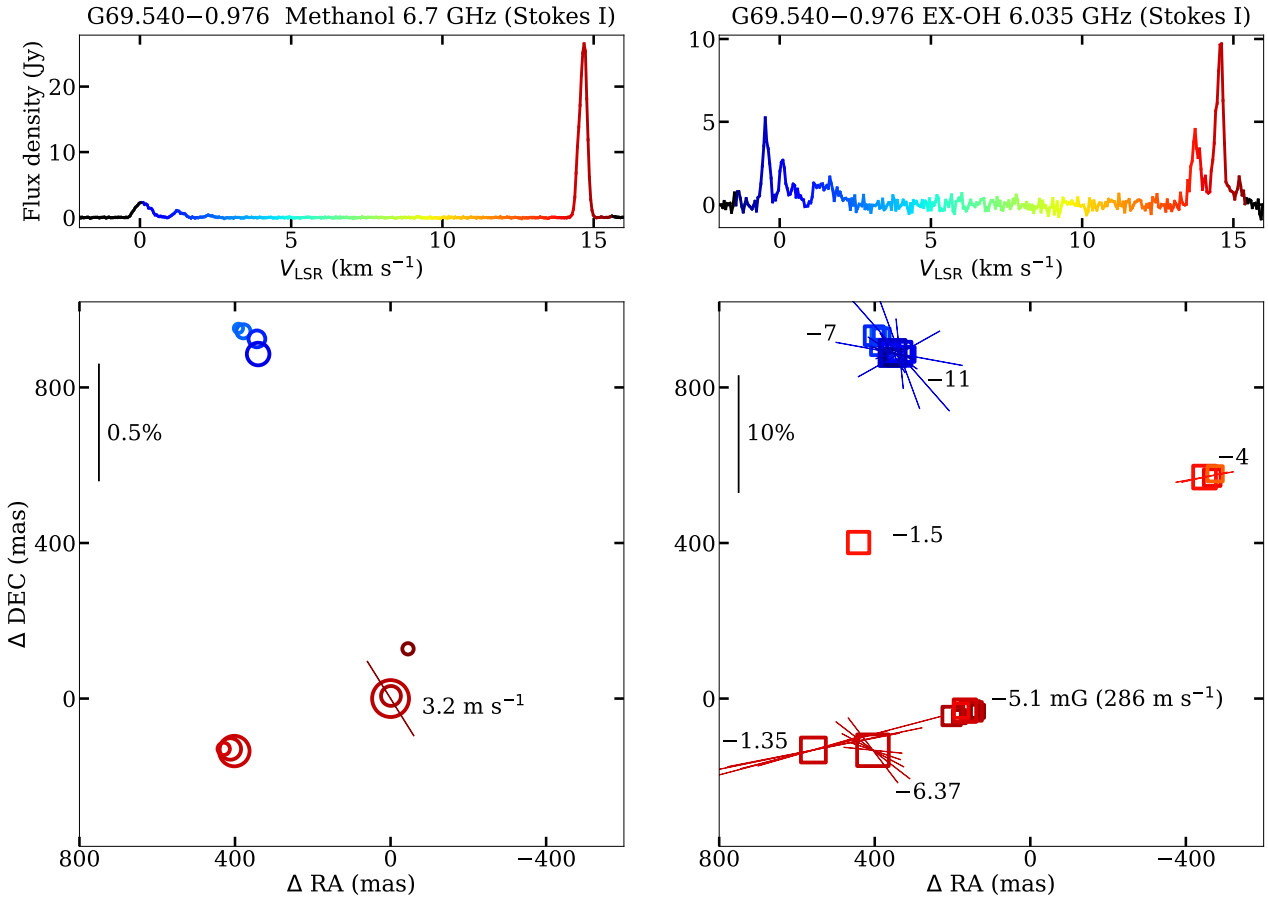

Fig. 1. The spectra (top panels) and maser distributions (bottom panels) of the 6.7 GHz methanol (left) and 6.035 GHz ex-OH masers (right) in ON 1, with linear polarization vectors and estimated Zeeman splitting (left) and magnetic field strength along the line-of-sight (right).

have $B_{||}^{meth} = -62.8$ mG for ON 1, and -41.2 mG and -23.5 mG for W75N. These values are a few times larger than the derived $B_{||}^{exOH}$, and in the case of the magnetic field in W75N an opposite sign is even seen. Now we can determine a density ratio between the two maser species by assuming the relation $|B| \propto (n_{H_2})^{0.5}$ (Crutcher & Kemball 2019), that is:

$$n_{H_2}^{exOH} = \left(\frac{|B_{||}^{exOH}|}{|B_{||}^{meth}|} \right)^{\frac{1}{0.5}} n_{H_2}^{meth} \quad (5)$$

From Eq. 5 we have $n_{H_2}^{exOH} = 0.007\ n_{H_2}^{meth}$ for ON1, and $n_{H_2}^{exOH} = 0.03\ n_{H_2}^{meth}$ or $n_{H_2}^{exOH} = 0.1\ n_{H_2}^{meth}$ for W75N. These density relations are in agreement with the expected density range for both maser transitions ($10^5 < n_{H_2}^{meth} < 2 \times 10^8$ cm^{-3} and $10^6 < n_{H_2}^{exOH} < 3 \times 10^8$ cm^{-3}; Cragg 2002). This might indicate that the hyperfine transition $F = 3 \rightarrow 4$ can be the favored one. However, since we obtained different gas density relations for both sources as well as different signs of the magnetic field from the two transitions in W75N, maybe $F = 3 \rightarrow 4$ is not always the favored hyperfine transition. Dall'Olio et al. (2020) suggested that the dominant hyperfine transition might also be either $F = 6 \rightarrow 7A$ ($\alpha_{Z,6\rightarrow 7A}^{meth} = +0.0117$ m s^{-1} G^{-1}) or $F = 7 \rightarrow 8$ ($\alpha_{Z,7\rightarrow 8}^{meth} = +0.0212$ m s^{-1} G^{-1}). Then, we obtain similar density relation to that in ON 1 if in W75N we consider for $\Delta V_Z^{meth} = 2.1$ m s^{-1} the transition $F = 7 \rightarrow 8$ ($B_{||}^{meth,7\rightarrow 8} = +99$ mG) and for $\Delta V_Z^{meth} = 1.2$ m s^{-1} the transition $F = 6 \rightarrow 7A$ ($B_{||}^{meth,6\rightarrow 7A} = +119$ mG).

In conclusion, there is not always a favored hyperfine transition for the 6.7 GHz methanol maser emission. In any case, we have that $B_{||}^{meth} >> B_{||}^{exOH}$ regardless of the chosen hyperfine transition, indicating that both masers may not arise in the same volume of gas.

Acknowledgements. The European VLBI Network (www.evlbi.org) is a joint facility of independent European, African, Asian, and North American radio astronomy institutes. Scientific results from data presented in this publication are derived from the following EVN project code EK052. AK, AB, MSz acknowledge support from the National Science Centre, Poland through grant 2021/43/B/ST9/02008.

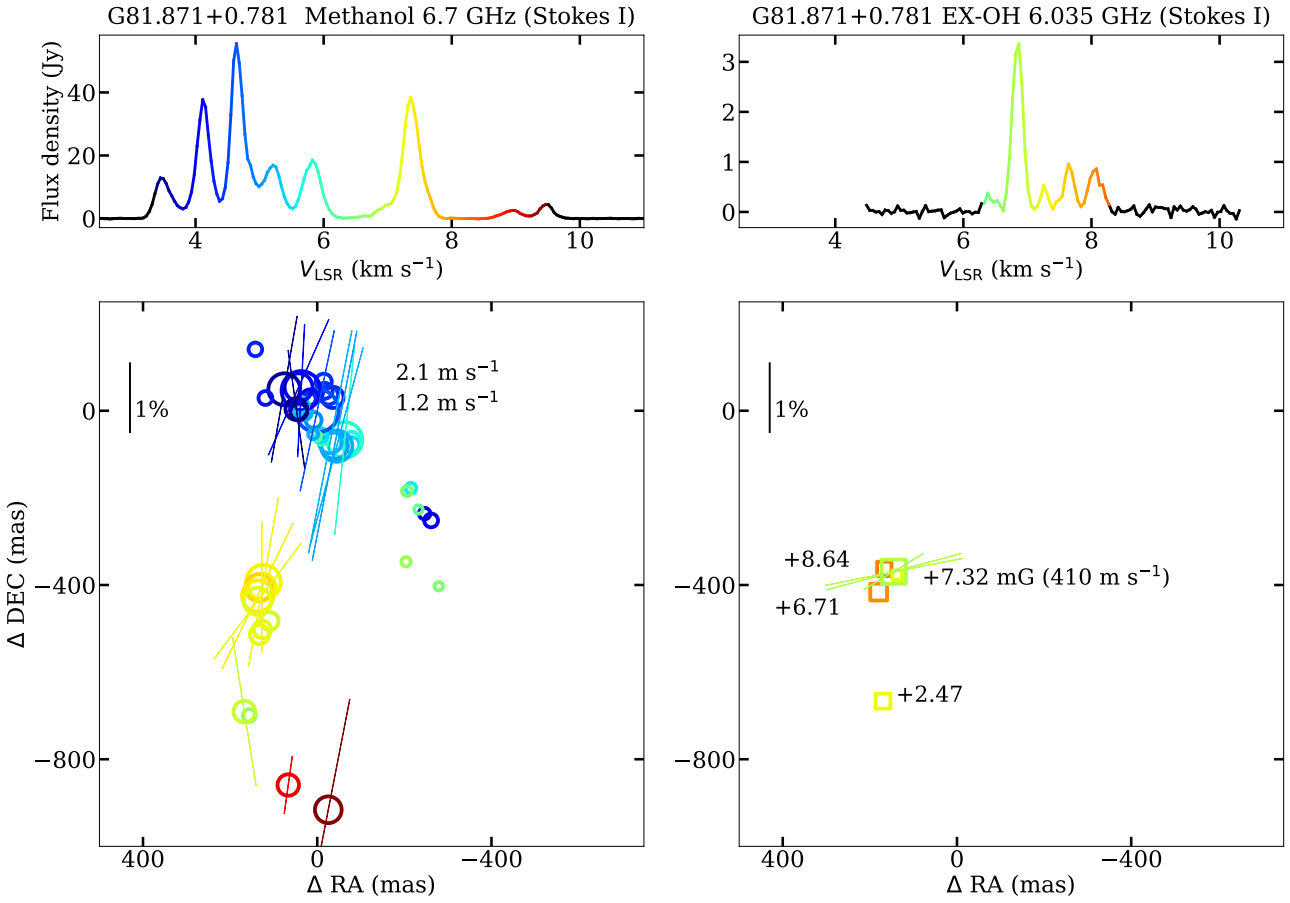

Fig. 2. Same as Fig. 1 but for W75N.

References

Avison, A., Quinn, L., Fuller, G. A., et al., 2016, MNRAS, 461, 136

Baudry, A., Desmurs, J. F., Wilson, T. L., et al. 1997, 325, 255

Caswell, J. L. 1996, 279, 79

Caswell J. L., 2003, MNRAS, 341, 551

Cragg, D. M., Sobolev, A. M., & Godfrey, P. D. 2002, 331, 521

Crutcher R. M. & Kemball A. J., 2019, Frontiers in Astronomy and Space Sciences, 6, 66

Dall'Olio, D., Vlemmings, W. H. T., Lankhaar, B., et al. 2020, A&A, 644, A122

Davies, R. D. 1974, in IAU Symposium, Vol. 60, Galactic Radio Astronomy, ed. F. J. Kerr & S. C. Simonson, 275

Ellingsen, S. P., Breen, S. L., Voronkov, M. A., et al. 2012, arXiv e-prints, arXiv:1210.2139

Etoka, S., Gray, M. D., & Fuller, G. A. 2012, MNRAS, 423, 647

Green, J. A., Caswell, J. L., & McClure-Griffiths, N. M. 2015, MNRAS, 451, 74

Hu, B., Menten, K. M., Wu, Y., et al. 2016, , 833, 18

Hutawarakorn, B., Cohen, R. J., & Brebner, G. C. 2002, MNRAS, 330, 349 1123

Jones, B. M., Fuller, G. A., Breen, S. L. et al., 2020, MNRAS, 493, 2015

Krumholz, M. R. & Federrath, C. 2019, Frontiers in Astronomy and Space Sciences, 6, 7

Lankhaar, B., Vlemmings, W., Surcis, G., et al. 2018, Nature Astronomy, 2, 145

Menten, K. M. 1991, , 380, L75

Pandian, J. D., Momjian, E., Xu, Y., et al. 2011, 730, 55

Rygl, K. L. J., Brunthaler, A., Reid, M. J., et al. 2010, , 511, A2

Rygl, K. L. J., Brunthaler, A., Sanna, A., et al. 2012, 539, A79

Surcis, G., Vlemmings, W. H. T., Curiel, S., et al. 2011, A&A, 527, A48

Surcis G., Vlemmings W. H. T., van Langevelde H. J., et al. 2022, A&A, 658, A78

Surcis G., Vlemmings W. H. T., van Langevelde H. J., et al. 2019, A&A, 623, A130

Szymczak M., Kus A. J., Hrynek G., et al. 2002, A&A, 392, 277

Szymczak M., Cohen R. J., Richards A. M. S., 2001, A&A, 371, 1012

Tan, J. C., Beltrán, M. T., Caselli, P., et al. 2014, in Protostars and Planets VI, ed. H. Beuther, R. S. Klessen, C. P. Dullemond, & T. Henning, 149–172

Vlemmings W. H. T., Surcis G., Torstensson K. J. E., et al. 2010, MNRAS, 404, 134